

## Detection of Cardiac Functions of Fetus with Diabetic Metabolic Disease through PEG-PCL Nano Micelle and Ultrasound Technique

Hongmei Ran<sup>1\*</sup>, Yunlong Zhang<sup>1</sup>, Dingding Yu<sup>2</sup>, Guoli Zhou<sup>3</sup>

<sup>1</sup>Department of Ultrasound, Linping District First People's Hospital, Hangzhou, 311100, China

<sup>2</sup>Department of Obstetrics, Linping District First People's Hospital, Hangzhou, 311100, China

<sup>3</sup>Department of Laboratory, Linping District First People's Hospital, Hangzhou, 311100, China

### ARTICLE INFO

#### Original paper

#### Article history:

Received: September 03, 2021

Accepted: March 02, 2022

Published: March 31, 2022

#### Keywords:

gestational diabetes; fetal ultrasound electrocardiogram; heart function; Tei index; PEG-PCL nano; ultrasound contrast agent

### ABSTRACT

The study was to probe into the application of ultrasound technique in gestational diabetes mellitus (GDM) and research the progress of PEG-PCL nano micelle and ultrasound technique. Method: 210 patients with a singleton pregnancy fetus, who received the fetal echocardiography in Yuhang District First People's Hospital from March 2019 to March 2020, were selected as the subjects, including 101 fetuses who were confirmed as gestational diabetes mellitus (GDM), and 109 normal fetuses (control group). The ultrasound cardiogram technique was employed to detect the thickness of the fetus ventricle septum, mitral/tricuspid annular displacement, left/right TEI indexes, and so on. The mean value of three cardiac cycles was taken as the test results. Finally, SPSS17.0 software was applied to the analysis of data. The nano micelle was made from the amphiphilic block copolymers (PEG-PCL) using the dialysis method/solvent evaporation method. The nanoscale ultrasound contrast agent was prepared from Decafluoropentane which was imaging gas. The characterizations were studied using the optical microscope, and transmission electron microscopy (TEM). The temperature sensitivity and ultrasound sensitivity of the nano-ultrasound contrast agent were analyzed with the particle size as the evaluation index. The in-vitro ultrasound contrast experiment was conducted to study the contrast-enhanced effect. Results: The fetal Tei index of the case group was higher than that of the control group, of which  $P < 0.05$  had statistical significance. However, the thickness of the fetus ventricle septum, Em, Am, and Em/Am of mitral/tricuspid annular were not significantly different from those of the control group ( $P > 0.05$ ). The nano ultrasonic contrast agent prepared through the ultrasonic injection method had a uniform particle size and a hollow shell-core structure under an electron projection microscope. The particle size of the nano-ultrasound contrast agent varied with temperature, and its microbubbles were generated under ultrasonic conditions. As compared with the blank degassed water group, a real linear echo appeared inside the contrast agent group, with small and even echo spots. The back echo remained with no obvious attenuation and lasted for a longer period. However, the blank degassed group had no distinct echo intensity and spot. Conclusion: PEG-PCL nano-ultrasound contrast agent achieved an excellent imaging effect; there was no obvious change to heart function and structure of the fetus, when gestational diabetes pregnant had blood sugar perfectly controlled, however, the fetus's heart function may change in the last trimester.

DOI: <http://dx.doi.org/10.14715/cmb/2022.68.3.4>

Copyright: © 2022 by the C.M.B. Association. All rights reserved.



### Introduction

Diabetes is one of the common complications during pregnancy, and about 7% of pregnant women will suffer from such a disease. Two common types of diabetes during pregnancy include pregestational diabetes mellitus (PGD), and gestational diabetes mellitus (GDM) (1). GDM is defined as the varying degrees of abnormal glucose tolerance occurred after pregnancy or for the first time, which is one of the severe risk factors during pregnancy. The research data shows that 80% of diabetes pregnant women get GDM (2). The incidence of GDM in China is 1.3-3.75%, and

its incidence in special populations attains 10-20% and shows a rising momentum year by year. GDM may exert adverse effects on mothers and fetuses (3). The clinical data shows that GDM can lead to the fetal congenital malformations, premature delivery, and a rise in perinatal morbidity and mortality, meanwhile, it may also result in abnormal metabolism of offspring, increasing the risk of obesity, growing probability of GDM in pregnant women with type 2 diabetes (4). PGDM means that the pregnant women are confirmed as diabetes patients before pregnancy. The clinical data shows that PGDM can cause fetal miscarriage and

\*Corresponding author. E-mail: [ncdx1209@163.com](mailto:ncdx1209@163.com)  
Cellular and Molecular Biology, 2022, 68(3): 24-33

malformations in early pregnancy, and congenital malformations of the fetal heart. The research data manifests that, over half of PGDM fetal deaths are arising from congenital malformations (5). The incidence of congenital malformations in PGDM fetuses is 4 times that of normal fetuses. In addition, the study shows that the incidence of cardiovascular malformations in PGDM is 5 times that of normal fetuses (6).

Because of the particularity of fetal anatomy and circulation, the evaluation of fetal heart function is more complicated than that of adults and children. Echocardiography has been extensively used in the diagnosis of fetal arrhythmia and vascular malformations due to its safety and non-invasive advantages (7). In recent years, with the development of perinatal technology, echocardiography technology is playing an increasingly important role in the diagnosis of fetal heart-related diseases (8). Congenital heart disease is the most common congenital malformation arising from diabetic pregnancy. Therefore, the echocardiography technology is very important for the detection of the fetal heart condition, and can intuitively reflect the growth and development of the fetus, and discover the abnormal fetal heart function before the fetal heart structure and function are changed (9), which provide a basis for obstetricians to perform the clinical intervention and select the appropriate delivery time (10). At present, more researches on the echocardiography of the heart function for gestational diabetes are mostly focused on PGDM patients, and fewer researches on the effects of GDM patients are conducted. Therefore, in this article, the GDM fetus was selected as the object, to further enrich the research on the effect of gestational diabetes on fetal heart function.

The ultrasound contrast agent is a critical part of ultrasound diagnostic technology (11). The ultrasound contrast agent (UCA) is able to remarkably enhance the echo signal, and greatly improve the image quality of tissues and organs, which exert an important role in the diagnosis of ultrasound (12). Nowadays, the common ultrasound contrast agent is a kind of micro-level & high-concentration microbubble preparation with a poor contrast effect. In order to raise the effect of ultrasound contrast agents, many scientists are committed to the research on nano-level ultrasound contrast agents (13). The research data showed that

PEG-PCL ultrasound nanobeams were featured by good biocompatibility and easy degradation, and were suitable to manufacture ultrasound contrast agents (14-16). In this article, the PEG-PCL ultrasound nanobeams were independently synthesized and prepared into ultrasound nano-contrast agents using imaging gas. Meanwhile, its contrast effect was also studied, in order to provide a basis for the research of more efficient and high-quality ultrasound contrast agents.

## **Materials and methods**

### **Subjects**

210 pregnant women who received the ultrasound examination in Yuhang District First People's Hospital from March 2019 to March 2020 were chosen as subjects. All pregnant women didn't have bad habits like smoking and drinking and had no history of chronic heart, liver, and kidney diseases. The results showed that all the fetuses' hearts were normal and got no arrhythmia. All patients were divided into the case group (101 patients) and control group (109) depending on the onsets of gestational diabetes. The pregnant women in the control group shall not have an apparent abnormality, and the fasting blood glucose (FBG) shall be less than 5.8mmol/L. The pregnant women in the case group shall meet the condition, in which their blood glucose could be controlled with no need to add insulin. All the subjects mentioned in this article signed the consent of inform and met the requirements for medical ethics.

### **Ultrasonic instrument and method**

The Philip IE33 color doppler ultrasonic diagnosis apparatus, with the probe model of S5-1 and S8-3, and the frequency of 1-5MHz and 3-8MHz, were adopted in this study. The parameters for fetus heart structure and hemodynamic parameters were obtained using M-type, 2D; color doppler, and tissue Doppler. Whether the fetus had abnormal heart structure was checked with the 2D echocardiography of the system; whether the fetus had the heart malformations were screened based on the four-chamber view, the outflow tract view, the long axis view of the aortic arch, and the color of blood flow chart. During all examinations, the fetus is required to keep breathless

and have no limb movements, and pregnant women are also required to hold their breath.

**Measurement of parameters**

[1] Thickness of ventricular septum: the M-type ultrasound cardiogram proceeded in the late ventricular diastolic phase. The sample line shall be perpendicular to the ventricular septum. If the thickness of the ventricular septum in the middle and late period of the pregnancy is  $\geq 5$ mm, such a case will be diagnosed as Hypertrophic Cardiomyopathy (HCM).

[2] DTI velocity frequency spectrum of mitral and tricuspid annulus motion: The apical four-chamber view is adjusted to DTI mode, and the volume of the sample is set to 2-5mm. The specific sampling positions are the roots of the posterior leaf of the mitral annulus and the roots of the anterior leaf of the tricuspid annulus. The specific Doppler spectrum is shown in Figure 1.

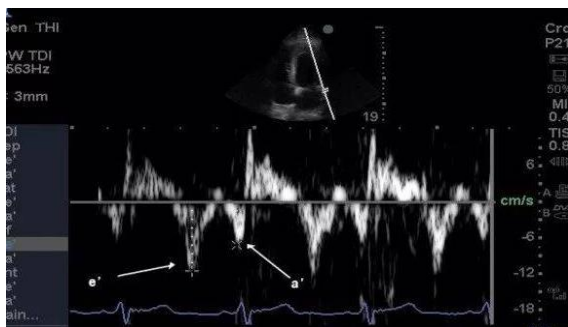


**Figure 1.** Ultrasonic cardiogram for the fetus, and dopplergram for tricuspid annular tissue

[3] Tei index is set as DIT pulse pattern, and sample solvent is set to 2-5mm. The sampling container is placed at the junction of the posterior mitral valve leaflet and its annulus, and the junction of the tricuspid valve and its annulus. The doppler sampling line shall be parallel to the motion direction of the atrioventricular valve. The scanning speed is 75-150mm/s. Figure 2 showed the measurement diagram for specific spectrum and Tei index of mitral and tricuspid annulus motion. There are Sm, Em, and Am waves in the mitral and tricuspid annulus. A indicates a section between the end of one Am to the start of the next Em wave, and b refers to the duration of the Sm wave. A-b is the sum of isovolumic contraction time (ICT) and isovolumic relaxation time (IRT), and b is

ejection time (ET). The calculation equation for Tei index is shown as  $(ICT+IRT)/ET$ .

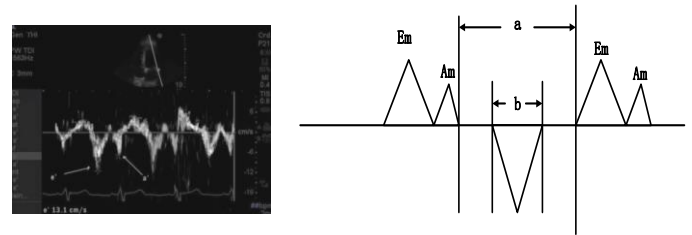


**Figure 2.** The schematic diagram for measurement of Tei index in ultrasound cardiogram

[4] Left Atrial shortening fraction (LASF): according to a 2D ultrasound cardiogram, the M-type measurement is conducted. The parasternal long-axis view is used, to ensure the sampling line is perpendicular to the interatrial septum in the middle of the left atrium. The calculation equation for LASF is shown as follows:  $(\text{left atrial diastolic diameter} - \text{left atrial diastolic diameter of systolic}) / \text{left atrial diastolic diameter of systolic}$ . The specific model diagram is shown in Figure 3.

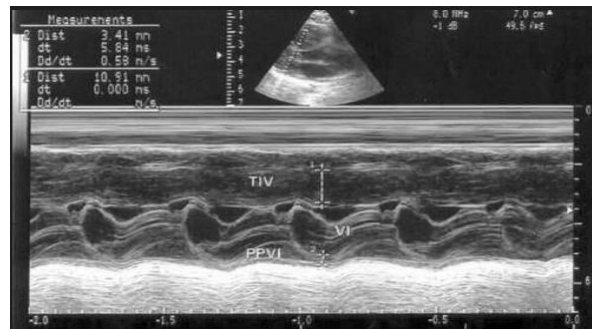


**Figure 3.** Measurement of shortening rate of left atrium short axis of the fetus

[5] The mitral annular displacement (MAD) and tricuspid annular displacement (TAD): the standard four-chamber view, and left and right ventricle display views, are measured using M-mode echocardiography. The sampling points are located at the left ventricular free wall, the mitral annular, and the junction of the tricuspid annular and the free wall of the right ventricle. The sound beam and the heart shall maintain longitudinal balance. The intersection angle should be below 20 degrees. The maximum distance from diastasis to the systole of the mitral and tricuspid annular is the maximum displacement of the mitral and tricuspid annular. The specific model diagram is shown in Figure 4.

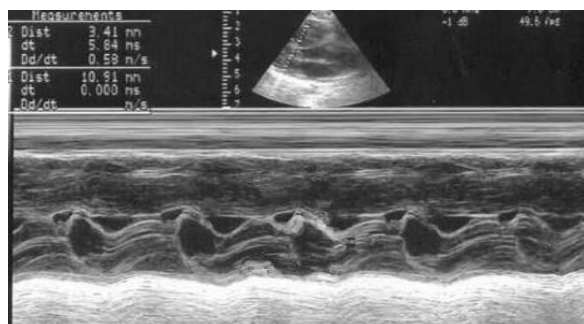


**Figure 4.** Measurement of maximum ultrasonic displacement of the tricuspid valve of the fetus

### Preparation of PEG-PCL nano-micelle & ultrasound contrast agent

50mg of PEG-PCL polymer were filled into 1mL of acetone organic solvent for uniform dissolution. The mixture was stirred with a magnetic stirrer and slowly dropped into a beaker containing 10mL of deionized water, and then stirred until the solvent was completely volatilized. The liquid collected was centrifuged for 10 minutes at 4000 rpm/10sec. The supernatant was collected, and filtered with a microporous membrane (0.45um). The filtrate collected was stored in a refrigerator at 4°C for later use.

### Related characterizations

The sample went through the negative staining, the polymer micelles were diluted to a certain concentration, dripped onto the carbon-coated copper mesh, and dried for 4 hours, and taken out. A drip of 2% phosphate should be filled in. The negative dyeing was absorbed with the filter paper after a minute. After being dried after two hours, its shape and size were observed under a transmission electron microscope. The particle size of the sample should be measured by Malvern.

### Study on contrast experiment

In-vitro contrast test: a certain amount of PEG-PCL nano-micelle ultrasound contrast agent was drawn using the syringe, and placed in a 37°C constant temperature water bath. The sponge anechoic layer with a thickness of 1cm adhered to the bottom of the water bath and the ultrasound probe was arranged in the water for ultrasound imaging. According to the imaging effect of the sample with initial concentration, the dilution factor was adjusted until

the image had no obvious attenuation and appeared a uniform and internal echo signal. The ultrasound conditions were consistent each time, and the degassing & double steaming group served as the control group.

In-vivo contrast test: 5 magnetic rats with a weight of 20-24g were prepared. 4ml/kg chloral hydrate (100g/L) was injected intraperitoneally. The body hair of the rat heart area was removed using the depilatory cream, and the rat was fixed to a wooden frame in the supine position and indwells a scalp needle in the tail vein. The mechanical index (MI) of the ultrasonic diagnostic apparatus was 0.6, the imaging depth was 3.5cm, and the rat heart ultrasound was collected at different time points before and after the injection of the contrast agent. Ultrasonic inspection parameters remained unchanged during the experiment.

## Results and discussion

### General information on patients

Table 1 showed the general information about the subjects. 210 pregnant women were included in the study and underwent 256 echocardiography examinations. 101 pregnant women were confirmed as GDM patients and the mean value of gestation period was 31.1. The mean value of the gestation period of 109 normal women was 30.9. Two groups of pregnant women were divided into 25-27, 28-33, and 34-38 weeks according to different gestation periods. Two groups of pregnant women had no apparent disparities in terms of age, parity, fetal heart rate (FHR) and so on.  $P > 0.05$  indicated no statistical significance.

**Table 1.** General information on subjects

Grouping of gestation period (weeks)	Case group (n=101)			Control group (n=109)		
	25-27	28-33	34-38	25-27	28-33	34-38
Number of cases	21	58	22	23	69	17
Age of pregnant women (years old)	22-39 (32±4.1)			24-33 (28±3.8)		
Gestation period	25-38(31.1±3.8)			25-38(30.9±3.1)		

### Comparison of the thickness of ventricle septum of two groups of fetuses

The thickness of the ventricle septum of two groups of fetuses varied with the gestation period, as shown in Figure 5. This figure manifested that, the ventricle septum of two groups of fetuses became thicker with

the increase in the gestation period.  $P < 0.01$  indicated the statistical significance. Two groups had no obvious disparities in the thickness of the ventricle septum during the whole gestation period. At 28-33 and 34-38 weeks, the thickness of the ventricle septum of the GDM group was slightly higher than that of the control group and had no remarkable differences.  $P > 0.05$  indicated no statistical significance.

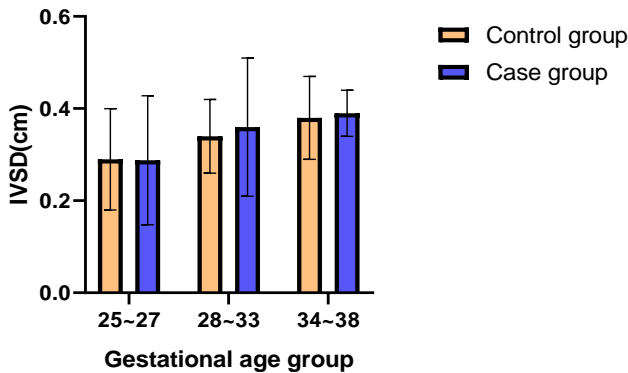


**Figure 5.** Variation of thickness of ventricle septum of two groups of patients with a gestation period

### Ventricular diastolic and contraction function of two groups of fetuses

Figures 6 and 7 showed the comparison results of left/right ventricular diastolic and contraction function of two groups of fetuses in different gestation periods. Figure 6 showed that Em, Am, and Em/Am of mitral/tricuspid annular of two groups of fetuses were growing with the increase of gestation period, and were divided into different groups according to gestation period. Such groups were compared.  $P < 0.05$  indicated the statistical significance; The AM of mitral/tricuspid annular of two groups of fetuses just had a slight growth with the increase of the gestation period. In terms of comparison in the group,  $P > 0.05$  indicated no statistical significance.

TAD and Mad of two groups of fetuses had a slight growth with the increase in the gestation period, however, in terms of comparison in the group,  $P < 0.05$  indicated no statistical difference; EF had no apparent disparity with the variation of the gestation period and was a lower correlation with the gestation period. All the indexes of the control group were slightly higher than those of the case group. However, in terms of comparison of parameter groups,  $P > 0.05$  indicated no statistical significance.

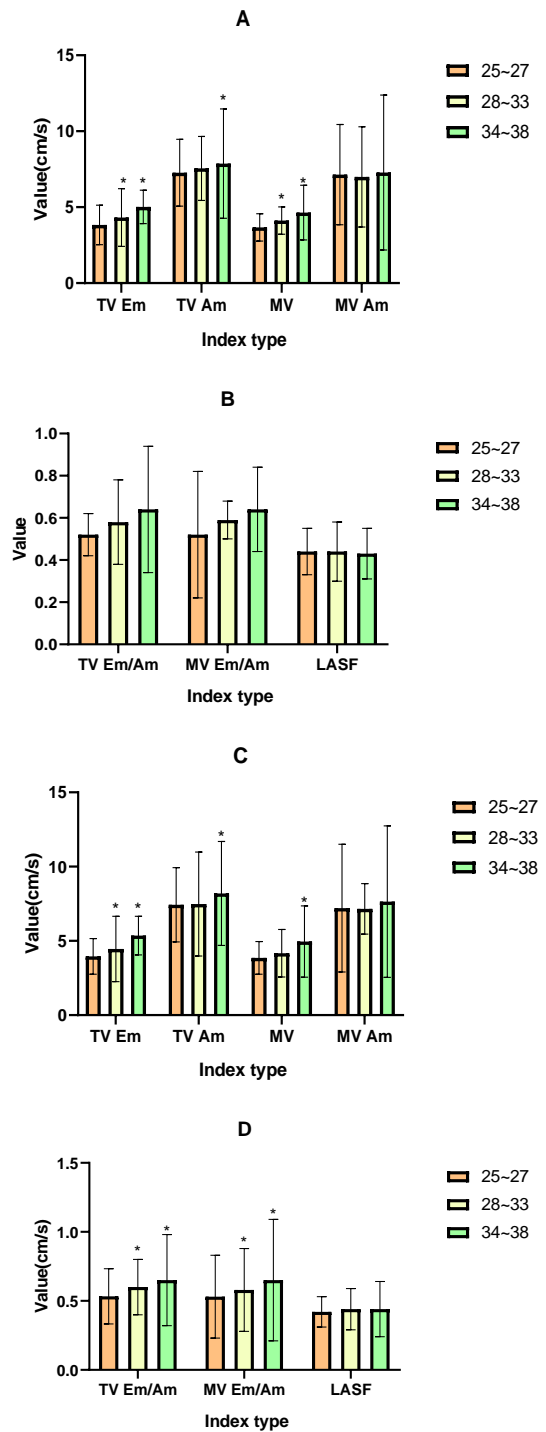


**Figure 6.** Indexes of ventricular diastolic function of two groups of fetuses. Note: \* meant  $P < 0.05$  compared with the results at 25 ~ 27 week. Notes: A and B represented the relevant indexes of the case group; C and D indicated the relevant indexes of the control group

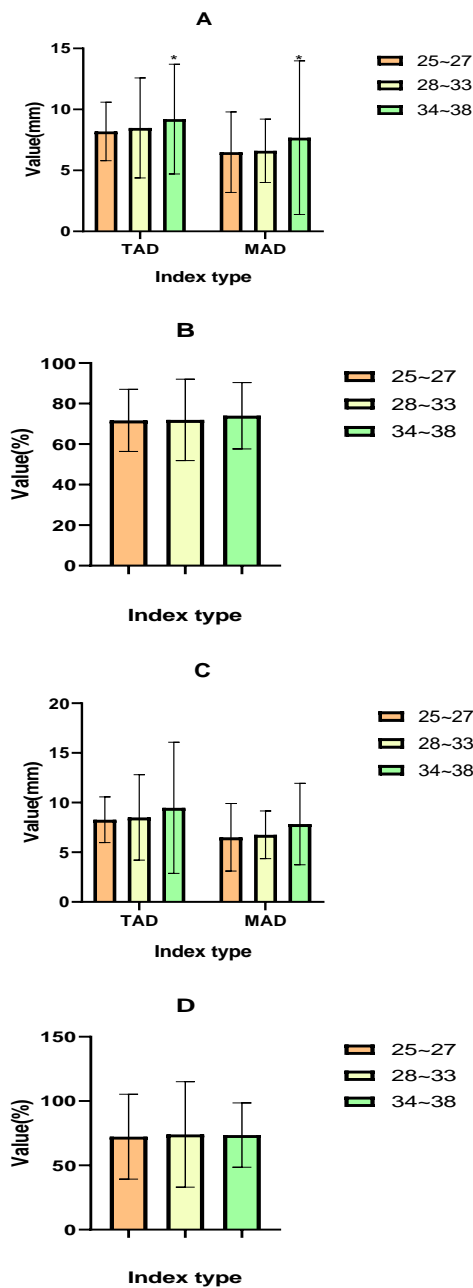


**Figure 7.** Indexes of ventricular contraction function of two groups of fetuses. Notes: A and B represented the relevant indexes of the case group; C and D indicated the relevant indexes of the control group

**Evaluation of the whole ventricular function of the fetus**

Figure 8 showed the evaluation of indexes of the whole ventricular function of the fetus. It was analyzed in Figure 8 that, the Tei indexes, ET, ICT+IRT of left/right fetus ventricular of the control groups had no major variation with the increase of the gestation period. In terms of comparison among groups,  $P < 0.05$  indicated no statistical significance; while Tei indexes and ET of left/right fetus ventricular of the case groups

had growth with the increase of the gestation period. In terms of comparison in the group,  $P < 0.05$  indicated the statistical significance; ICT+IRT had no apparent variation with changing gestation period ( $P > 0.05$ ). The Tei indexes, ICT+IRT, and ET of two groups of fetuses in the whole gestation period were compared,  $P < 0.05$  indicated no statistical significance; after 34-38-week gestation period, the Tei indexes of left/right fetus ventricular of the case groups were higher than those of the control groups.  $P < 0.05$  indicated the statistical significance.

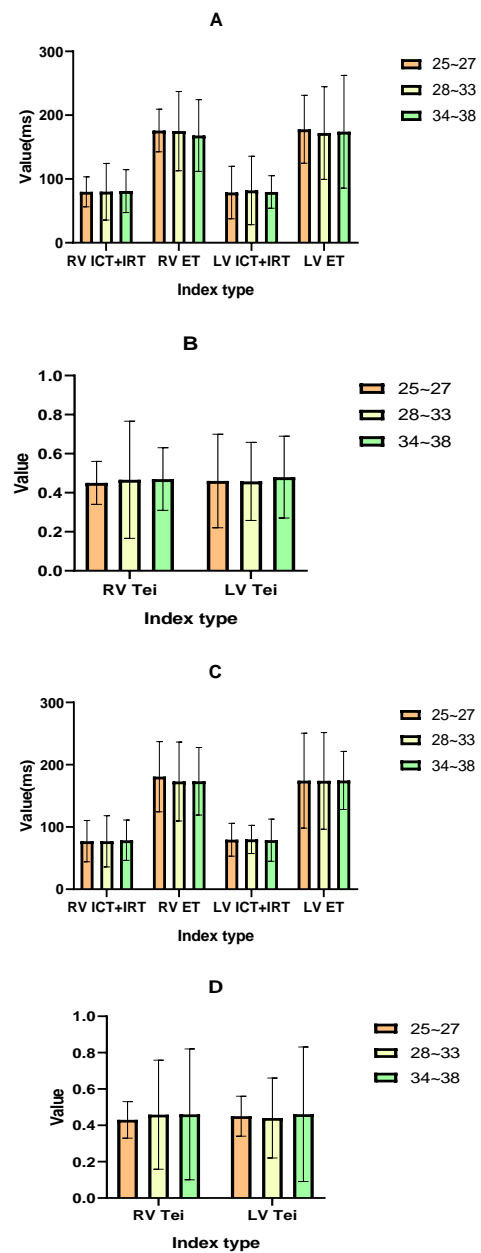


**Figure 8.** Evaluation of indexes for the whole ventricular function of two groups of fetuses. Notes: A and B represented the parameters for case group; C and D indicated parameters for the control group

### Characterization of EG-PCL Nano-micelle ultrasound contrast agent and measurement results of particle size

Figure 9 showed the transmission electron microscope (TEM) images for EG-PCL nano-micelle and ultrasound contrast agent, and measurement results of particle size. Figure 9 manifested that, the hydrophobic segment of the polymer micelle was dyed into a white kernel with wolfram phosphoric acid, and the PEG shell presented a gray aureole because it adsorbed part of the wolfram phosphoric acid in the water. The micelles had a spherical kernel-shell structure with a uniform size. The measurement results of Malvern particle size showed that the average particle size was consistent with the results of the TEM.

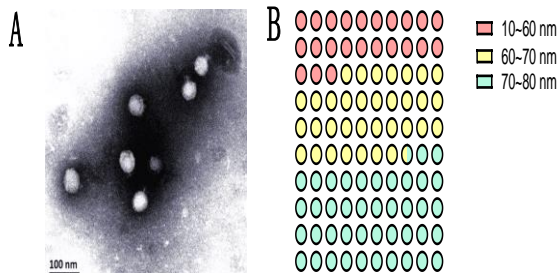


**Figure 9.** Transmission electron microscope (TEM) images for EG-PCL nano-micelle and ultrasound contrast agent, and measurement results of particle size. Notes: A indicated the transmission electron microscope scan; B represented the distribution of particle sizes

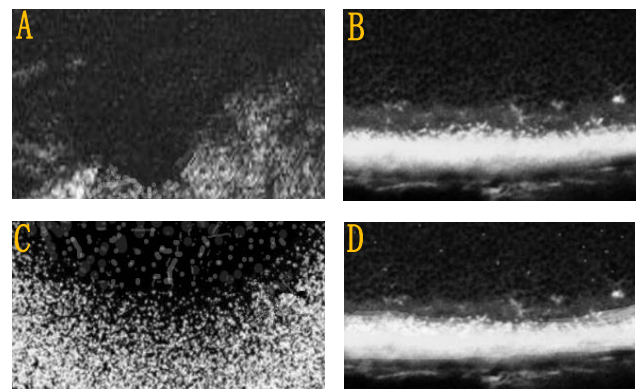
### In-vitro contrast experimental results

Figure 10 showed that the ultrasound images for the contrast agent group and the control group. A and B represent the ultrasound images for the degassed water group in an ultrasound mode and 2D mode; C and D indicate the ultrasound images for the contrast agent group in an ultrasound mode and 2D mode. Figure 11 showed that when the EG-PCL nanomicelle ultrasound contrast agent entered the development area, and achieved an effect, with the internal solid echo, and had a small and uniform light spot, and slight back echo attenuation; while the degassed water group had no echo.

### Contrast experimental results of animals

Figure 11 showed that the dynamic ultrasound contrast results for rat hearts. A and B represented the images in the ultrasound and 2D mode after 180

minutes; C and D indicated the images in ultrasound and 2D mode in 50 minutes after injection of contrast agent; E and F represented images in ultrasound and 2D mode in 120 minutes after injection of contrast agent; G and H indicated the images in ultrasound and 2D mode in 180 minutes after injection of contrast agent. Figure 11 showed that, the ultrasonic echo intensity was growing as the injection time of contrast agent was rising. The ultrasound echo didn't emerge upon the injection of contrast agent. The substantial echo was increasingly intensified after 30 minutes, and had maximum intensity after 50 minutes. The substantial enhanced echo may last for 3 hours.



**Figure 10.** Two groups of ultrasound mode and ultrasonography in 2D modes. Notes A and B: Dehydrating ultrasound and 2D Ultrasonography; Notes C and D indicate the contrast agent group and 2D mode

Diabetes is one of the common complications during pregnancy (17). Diabetes during pregnancy falls into the PGDM and GDM. GDM is defined as the varying degrees of abnormal glucose tolerance occurred after pregnancy or for the first time, which is one of the severe risk factors during pregnancy. The research data shows that 80% of diabetes pregnant women get GDM (18). The incidence of GDM in China is 1.3-3.75%, and its incidence in special populations attains 10-20% and shows a rising momentum year by year. GDM may exert adverse effects on mothers and fetuses (19). The clinical data shows that GDM can lead to the fetal congenital malformations, premature delivery, and a rise in perinatal morbidity and mortality, meanwhile, it may also result in abnormal metabolism of offspring, increasing the risk of obesity, growing probability of GDM in pregnant women with type 2 diabetes (20). PGDM means that the pregnant women are confirmed as diabetes patients before pregnancy, and can easily

cause the fetal miscarriage and malformations in early pregnancy, and congenital malformations of the fetal heart. Its influence on the heart may easily result in congenital malformation and cardiovascular anomalies. At present, the researches on diabetes during pregnancy were mostly focused on PGDM. In this article, GDM pregnant women were selected as the subjects, to expand the relevant studies on the diabetes of fetuses during pregnancy.

Because of the particularity of fetal anatomy and circulation, the evaluation of fetal heart function is more complicated than that of adults and children. Echocardiography has been extensively used in the diagnosis of fetal arrhythmia and vascular malformations due to its safety and non-invasive advantages. In recent years, with the development of perinatal technology, echocardiography technology is playing an increasingly important role in the diagnosis of fetal heart-related diseases. Congenital heart disease is the most common congenital malformation arising from diabetic pregnancy (21). Therefore, the echocardiography technology is very important to the detection of the fetal heart condition, and can intuitively reflect the growth and development of the fetus, and discover the abnormal fetal heart function before the fetal heart structure and function are changed, which provides a basis for obstetricians to perform the clinical intervention and select the appropriate delivery time (22). In this article, various indicators in ultrasound echocardiography of GDM and their influence on heart function were studied. The study showed that various indicators were related to the occurrence of DGM, especially the Tei index.

Nanotechnology can open new windows for various sections of biomedicine (23-25). The ultrasound contrast agent is a critical part of ultrasound diagnostic technology. The ultrasound contrast agent (UCA) is able to remarkably enhance the echo signal, and greatly improve the image quality of tissues and organs, which exert an important role in the diagnosis of ultrasound (26). Nowadays, the common ultrasound contrast agent is a kind of micro-level & high-concentration microbubble preparation with a poor contrast effect. In order to raise the effect of ultrasound contrast agents, many scientists were committed to the research on nano-level ultrasound contrast agents (27).

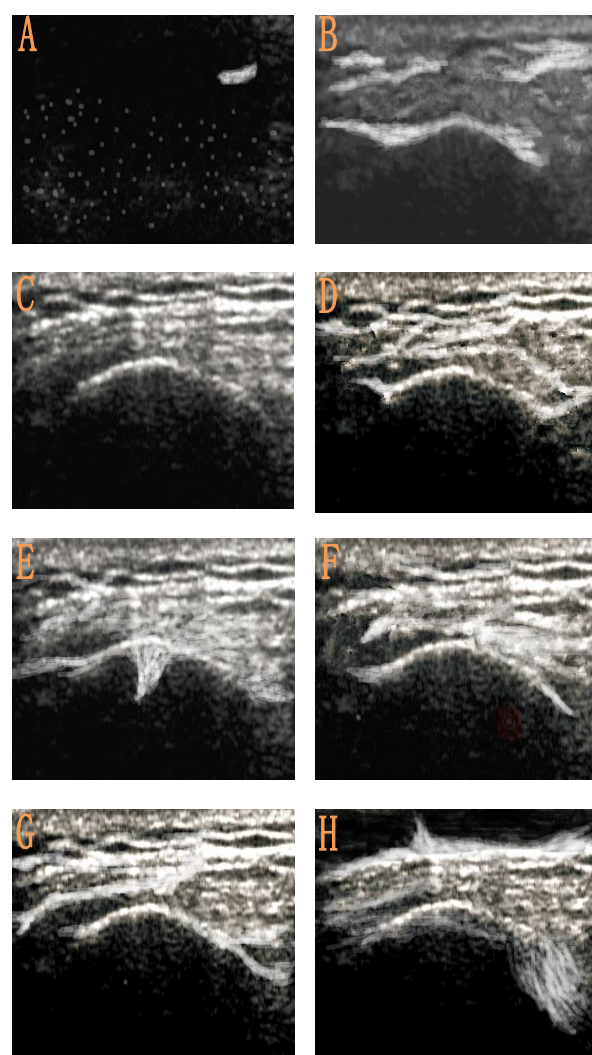


**Figure 11.** Dynamic ultrasound contrast-detection results for rat heart after injection of contrast agent

The research data showed that PEG-PCL ultrasound nanobeams featured good biocompatibility and easy degradation, and were suitable to manufacture ultrasound contrast agents (26). In this article, the PEG-PCL ultrasound nanobeams were independently synthesized and their contrast effect was also studied, which showed that the PEG-PCL ultrasound contrast had a good effect.

### Conclusion

In this article, various indicators in echocardiography of GDM fetuses and their significance in the evaluation of heart function of GDM fetuses were studied. The results showed that various indicators in ultrasound echocardiography had certain instructive significance in the evaluation of heart function of GDM fetuses, like the Tei index. Moreover, in this article, the PEG-PCL ultrasound contrast agent

was independently synthesized and its contrast effect was studied. The study showed that the PEG-PCL ultrasound contrast had a good effect. This article provided a basis for the research on PEG-PCL nanomicelle & ultrasound in terms of the evaluation of heart function of GDM fetuses. However, the article still has many shortcomings. For example, the article has no adequate samples, and the research on ultrasound contrast agents is still limited to animal experiments. The issue will be studied further in the latter study and work.

### Acknowledgments

None

### Conflict interest

The authors declare no conflict of interest.

### References

1. Mohsin M., Sadqani S., Younus K., Hoodbhoy Z., Ashiqali S., Atiq M. Evaluation of cardiac function in fetuses of mothers with gestational diabetes. *Cardiol Young* 2019;29(10):1264-1267.
2. Moore-Morris T., van Vliet P.P., Andelfinger G., Puceat M. Role of Epigenetics in Cardiac Development and Congenital Diseases. *Physiol Rev* 2018;98(4):2453-2475.
3. Gibb A.A., Hill B.G. Metabolic Coordination of Physiological and Pathological Cardiac Remodeling. *Circ Res* 2018;123(1):107-128.
4. Leszczynska K., Meyer-Szary J., Chojnicki M., Haponiuk I., Preis K., Stefanska K., Gierat-Haponiuk K., Swiatkowska-Freund M. Evaluation of cardiac function in donor and recipient fetuses during a 7-day follow-up after selective laser photocoagulation of communicating vessels due to TTTS. *Ginekol Pol* 2019;90(4):189-194.
5. Gebuza G., Zaleska M., Kazmierczak M., Mieczkowska E., Gierszewska M. The effect of music on the cardiac activity of a fetus in a cardiotocographic examination. *Adv Clin Exp Med* 2018;27(5):615-621.
6. Nakata M., Sakuma J., Takano M., Nagasaki S. Evaluation of fetal cardiac function with echocardiography. *J Obstet Gynaecol Res* 2020;46(1):31-38.
7. Meilhac S.M., Buckingham M.E. The deployment of cell lineages that form the mammalian heart. *Nat Rev Cardiol* 2018;15(11):705-724.
8. Alsolai A.A., Bligh L.N., Greer R.M., Kumar S. Correlation between fetoplacental Doppler indices and measurements of cardiac function in term fetuses. *Ultrasound Obstet Gynecol* 2019;53(3):358-366.
9. Cui Y., Zheng Y., Liu X., Yan L., Fan X., Yong J., Hu Y., Dong J., Li Q., Wu X., Gao S., Li J., Wen L., Qiao J., Tang F. Single-Cell Transcriptome Analysis Maps the Developmental Track of the Human Heart. *Cell Rep* 2019;26(7):1934-1950.e5.
10. McBrien A., Hornberger L.K. Early fetal echocardiography. *Birth Defects Res* 2019;111(8):370-379.
11. Turner J.M., Mitchell M.D., Kumar S.S. The physiology of intrapartum fetal compromise at term. *Am J Obstet Gynecol* 2020;222(1):17-26.
12. Tan C.M.J., Lewandowski A.J. The Transitional Heart: From Early Embryonic and Fetal Development to Neonatal Life. *Fetal Diagn Ther* 2020;47(5):373-386.
13. Pruetz J.D., Miller J.C., Loeb G.E., Silka M.J., Bar-Cohen Y., Chmait R.H. Prenatal diagnosis and management of congenital complete heart block. *Birth Defects Res* 2019;111(8):380-388.
14. Baschat A.A. Planning management and delivery of the growth-restricted fetus. *Best Pract Res Clin Obstet Gynaecol* 2018;49:53-65.
15. Patey O., Carvalho J.S., Thilaganathan B. Perinatal changes in cardiac geometry and function in growth-restricted fetuses at term. *Ultrasound Obstet Gynecol* 2019;53(5):655-662.
16. MacGrogan D., Münch J., de la Pompa J.L. Notch and interacting signalling pathways in cardiac development, disease, and regeneration. *Nat Rev Cardiol* 2018;15(11):685-704.
17. Loughran A.J., Orihuela C.J., Tuomanen E.I. *Streptococcus pneumoniae*: Invasion and Inflammation. *Microbiol Spectr* 2019;7(2):10.1128/microbiolspec.GPP3-0004-2018.
18. García-Otero L., López M., Guitart-Mampel M., Morén C., Goncé A., Esteve C., Salazar L., Gómez O., Martínez J.M., Torres B., César S., Garrabou G., Crispi F., Gratacós E. Cardiac and mitochondrial function in HIV-uninfected fetuses exposed to antiretroviral treatment. *PLoS One* 2019;4, 14(3):e0213279.
19. Basu M., Garg V. Maternal hyperglycemia and fetal cardiac development: Clinical impact and underlying mechanisms. *Birth Defects Res* 2018;110(20):1504-1516.

20. Eschbach S.J., Gijtenbeek M., van Geloven N., Oepkes D., Haak M.C. Measurement of cardiac function by cardiac time intervals, applicability in normal pregnancy and twin-to-twin transfusion syndrome. *J Echocardiogr* 2019;(3):129-137.
21. Alavi M, Webster TJ. Recent progress and challenges for polymeric microsphere compared to nanosphere drug release systems: Is there a real difference?. *Bioorg Med Chem*. 2021;33:116028.
22. Mohammed AK, Salh KK, Ali FA. ZnO, TiO<sub>2</sub> and Ag nanoparticles impact against some species of pathogenic bacteria and yeast. *Cellular and Molecular Biology* 2021;67(3):24-34.
23. Alavi M, Adulrahman NA, Haleem AA, Al-Râwanduzi ADH, Khusro A, Abdelgawad MA, et al. Nanoformulations of curcumin and quercetin with silver nanoparticles for inactivation of bacteria. *Cellular and Molecular Biology* 2022;67(5):151-6.
24. Jatavan P., Lerthiranwong T., Sekararathi R., Jaiwongkam T., Kumfu S., Chattipakorn N., Tongsong T. The correlation of fetal cardiac function with gestational diabetes mellitus (GDM) and oxidative stress levels. *J Perinat Med* 2020;48(5):471-476.
25. Morris G.M., Ariyaratnam J.P. Embryology of the Cardiac Conduction System Relevant to Arrhythmias. *Card Electrophysiol Clin* 2019;(3):409-420.
26. Wang J., Liu S., Heallen T., Martin J.F. The Hippo pathway in the heart: pivotal roles in development, disease, and regeneration. *Nat Rev Cardiol* 2018;(11):672-684.